CrystEngComm

Ambient *L*-Lactic Acid Crystal Polymorphism

Journal:	*CrystEngComm*
Manuscript ID	CE-COM-02-2021-000285.R1
Article Type:	Communication
Date Submitted by the Author:	20-Mar-2021
Complete List of Authors:	Yang, Jingxiang; New York University, Department Chemistry and Molecular Design Institute Reiter, Ethan; New York University, Chemistry and Molecular Design Institute Hu, Chunhua; New York University, Department of Chemistry Kahr, Bart; New York University, Department Chemistry and Molecular Design Institute

CrystEngComm

COMMUNICATION

Ambient *L*-Lactic Acid Crystal Polymorphism

Jingxiang Yang[a], Chunhua T. Hu [a], Ethan Reiter [a], and Bart Kahr* [a]

Received 00th February 2021,
Accepted 00th XXX 2021

DOI: 10.1039/x0xx00000x

www.rsc.org/23

Only one crystalline phase of the metabolite, *L*-Lactic acid (LLA), has been described since its isolation from sour milk as long ago as 1780. Herein, we report the structures of two new crystalline polymorphs of LLA obtained from supercooled melts and characterized by X-ray diffraction and micro-Raman spectroscopy, as well as their transformations from one phase to another. None of the three crystal structures are consistent with the aggregate geometries of LLA in cold matrices, in solution, or those predicted by quantum chemical computations. The latter aggregates feature typical cyclic carboxylic acid dimers not represented in any of the crystal structures. These differences underscore the difficulty of reasoning solid state structure from associations in other media.

L-Lactic acid (LLA, (*S*)-(+)-2-hydroxypropionic acid), "the grim harbinger of fatigue," according to Primo Levi,[1] may seem like a fatiguing subject in 2021 given the long scrutiny of glucose metabolism. Nevertheless, LLA has acquired verve in the last generation, now recognized in cellular signaling processes, immunity, memory formation, and cancer growth, among other essential processes of life and its decline.[2, 3] We have even learned that LLA is *not* responsible for muscle fatigue. This responsibility is just physiology folklore after all.[4] Meanwhile, industries manufacture LLA as a food additive[5] and as the precursor of the biodegradable poly(*L*-lactic acid)).[6] This wealth of LLA chemistry has prompted spectroscopic and computational investigations of self-association.[7,8,9,10] Here, we ask what story of LLA aggregation is told by crystallography?

Even though there is no end to sour milk, Scheele's source of lactic acid in 1780,[11] crystallization of LLA has been a challenge.[12] LLA crystals are highly hygroscopic[13] and they self-esterify,[14] confounding X-ray analysis.[15] The first single crystal structure of LLA, which we designate as polymorph Form **I** (CSD refcode YILLAG) , did not appear until 1994.[16] The crystal structure of Form **I** was redetermined here at 100K: space group $P2_12_12_1$, Z=4, Z'=1, a = 5.4954(4) Å, b = 8.4298(5) Å, c = 9.3517(6) Å, V = 433.22(5) Å^3, (Figure 2A). Form **I** was predicted to undergo a phase transition under isotropic pressure at *ca*. 1.03 GPa. [17] The computed high-pressure structure can be found in the CSD (refcode WUSWAL). We will designate it Form **IP**, as it was derived from Form **I** under simulated pressure.

Here, we report the discovery of two hitherto unknown polymorphs, Forms **II** and **III**. The crystal structures of Forms **II** and **III** were obtained from large, faceted single crystals (see Figures 1 and S2 for habits) harvested from supercooled melts.

Crystallization of LLA from solutions of ethanol, acetone, methyl propionate, ethyl acetate, acetic acid, diethyl ether, and tetrahydrofuran, only gave Form **I** as evidence by Raman microscopy. Melt crystallization has been an effective method of late for discovering new polymorphs.[18,19,20,21,22,23,24] LLA, however, when melted in sealed glass tubes and then quenched at 25 °C, gave no evidence of crystallization for more than 20 months. To induce expeditious nucleation of LLA, the thermodynamic driving force was increased by treating LLA melted between glass slides with dry ice (-78 °C) for about five minutes. Shortly after incubation at 25 °C, the growth of well-defined LLA spherulites was observed (Figure 1A). Micro-Raman spectroscopy was not consistent with Form **I** nor with a hydrate (Figure 2D, Figure S1). We designated this material polymorph Form **III** (Figure 2C). (We will return to the discovery of Form **II**, of intermediate thermodynamic stability). Form **III** melted at 32 °C, as compared with Form **I** at 53 °C). Low-melting, hygroscopic Form **III** did not survive attempts to measure its powder X-ray diffraction (PXRD) pattern, however.

[a] *Department of Chemistry, New York University, 100 Washington Square East Room 1001, New York, NY 10003, USA.*
Electronic Supplementary Information (ESI) available: [details of any supplementary information available should be included here]. See DOI: 10.1039/x0xx00000x

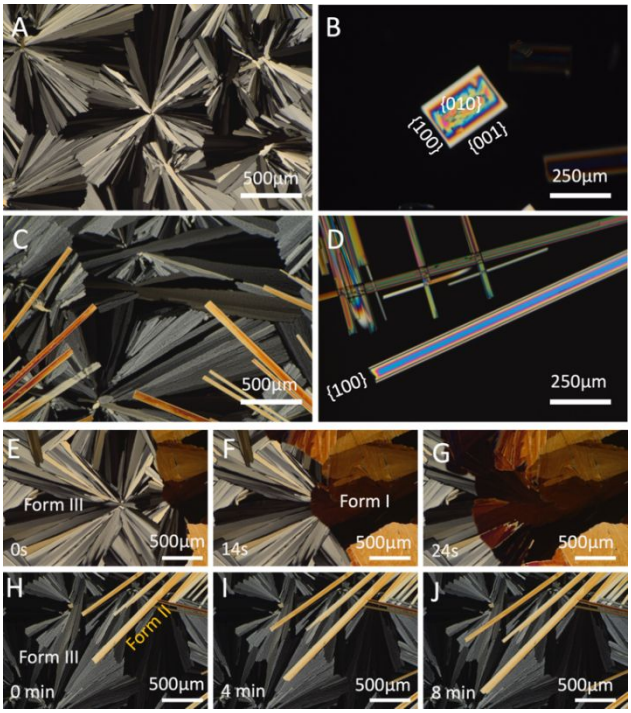

Fig. 1 (A) Spherulites of LLA **III**. (B) A single crystal of LLA **III** grown in a melt at 30 °C. (C) LLA **II** fibres (orange interference colour) growing in the spherulitic film of **III**. (D) A single crystal of LLA **II** grown in a melt at 34 °C. (E-G) Phase transformation of **III** to **I** at 25 °C. (H-J) Phase transformation of **III** to **II** at 25 °C.

Large, principally faceted single crystals of Form **III** were harvested from partially melted spherulites after 2-3 hours of incubation at 30 °C (Figure 1B, Figure S2B). These substantial crystals (>250 μm in the largest dimension) subsequently were cooled with dry ice and protected by an atmosphere of liberated CO_2. A crystal was removed from the surrounding glass with an X-ray loop and immediately placed on a goniometer in a stream of N_2 gas at 100 K. The crystals of Form **III** were consistent with the space group $P2_12_12_1$, like Form **I**, but with Z'=2, a = 5.7323(3) Å, b = 9.0190(5) Å, c = 17.33579(10) Å, V = 897.49(9) Å^3 (Figure 2C, Table S1). The two independent molecules are identified as m1 and m2 in Figures 3 and 4.

In addition to the spherulites and rectangular prisms of Form **III**, thin fibers often grew (Figure 1C). These fibers did not melt at 33 °C (one degree above the melting point of Form **III**) and grew as individual crystallites as opposed to polycrystalline spherulites. Micro-Raman spectroscopy revealed that the needles were neither Form **I** nor Form **III**, suggesting the presence of yet another polymorph, herein designated as Form **II** (Figure 2D, Figure S1). One needle of Form **II** (Figure 1D, Figure S2A) was excised from the melt for single crystal X-ray structure determination. Form **II** also crystallized in $P2_12_12_1$ yet again, Z'=1, a = 5.759(3) Å, b = 5.772(3) Å, c = 12.492(7) Å, V = 415.246(4) Å^3 (Figure 2B, Table S1).

The thermodynamic stabilities of LLA polymorphs were evaluated by melting points and phase transformations. The melting points of Forms **I**, **II**, and **III** are 53 °C, 36 °C, 32 °C, respectively, with thermodynamic stability decreasing as **I** > **II** > **III**. Transformations among all three polymorphs were studied via both optical microscopy and micro-Raman spectroscopy.

When confined between glass slides at 25 °C, Form **III** remained stable for weeks until it deliquesced (providing that it did not contact Forms **I** and **II**). However, concomitant crystallization of Forms **II** and **III** led to the transformation of **III** to **II** (Figure 1H-J). Upon contact, both Forms **II** and **III** transformed to **I** within minutes (Figure 1E-G). No reversible transformation was observed.

Curiously, the densities measured at 100K, did not follow the thermodynamic stabilities of the Forms above room. temperature. **III** was the densest and **II** the least dense. However, as we know from ice and water, this is not impossible for phases rich in H-bonds.

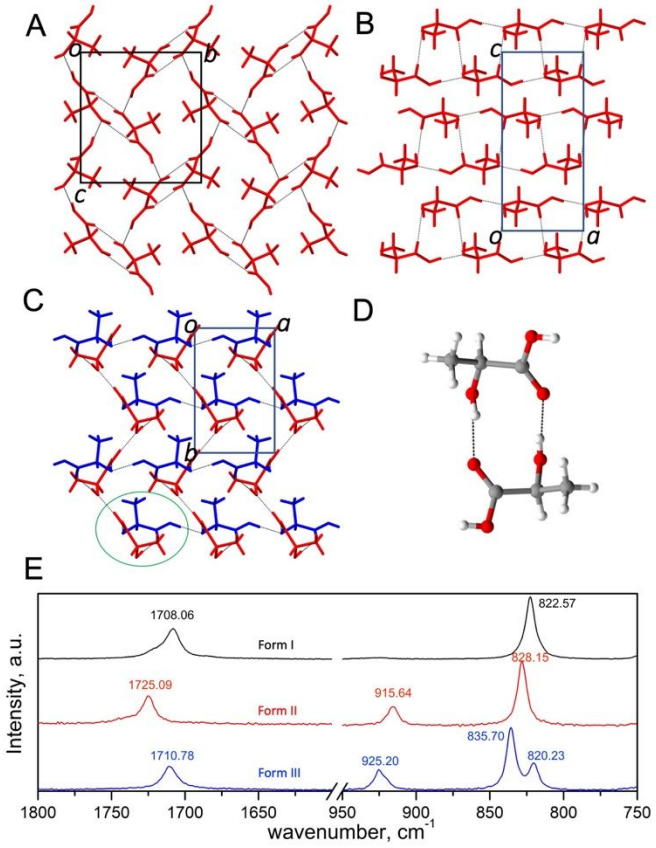

Fig. 2 (A) Crystal structure of LLA in Form **I**. (B) Parallel 2D hydrogen-bonded ribbons composed by $R_3^3(11)$ rings in Form **II**. (C) Hydrogen-bonded sheets in Form **III**, a pair of hydrogen-bonded -O=C-C-OH- $R_2^2(10)$ dimers (D). (E) Raman spectra of LLA polymorphs.

The theoretical conformations of LLA monomers were previously reported.[7,15,25,26,27] With the newly discovered polymorphs **II** and **III**, we now have four crystallographic conformations instead of just one (Figure 3A). The conformations differ in the C1-C2-O3-H3 dihedral angle (Figure 3B,C), *anti* as opposed to *syn* with respect to the methyl group. The conformer of LLA in Form **I** is geometrically closest to the conformer *AsC* (see ref 26 for nomenclature) which is *ca*. 19 kJ/mol higher than the *SsC* ground state in the gas phase. *Asc* is not expected to be measurably populated as this conformer is short by one hydrogen bond, otherwise satisfied in the crystalline states. *SsC*, detected in the gas phase by microwave[15]

and infrared spectroscopies,[10] is similar to conformers of Forms **II** and **III** (Fig. 3C).

LLA Form **I** molecules are bonded to three adjacent, symmetry-related molecules through a 3D hydrogen bond network (Figure 2A), resulting in ring structures, including $R_1^2(5)$, $R_6^5(18)$, $R_6^5(24)$, $R_6^6(26)$, as described by the language of graph sets.[28,29] In Form **II**, the hydrogen bond network can be characterized as $R_3^3(11)$. Rings further propagate along the *a*-axis to form 2D ribbons (Figure 2B). The same chain structure is also seen in *L*-alanine (CSD refcode, LALNIN55[30]), for example. In Form **III** (Figure 2C), one symmetry-independent molecule (blue) extends as a 1D chain along the *a*-axis, with the other molecule (red) extending as a 1D, zigzag chain along *b*; two symmetry-independent molecules are connected to each other by a pair of hydrogen bonds, forming -O=C-C-OH- $R_2^2(10)$ dimers (Figure 2D), further resulting in a hydrogen-bonded sheet in the (001) plane.

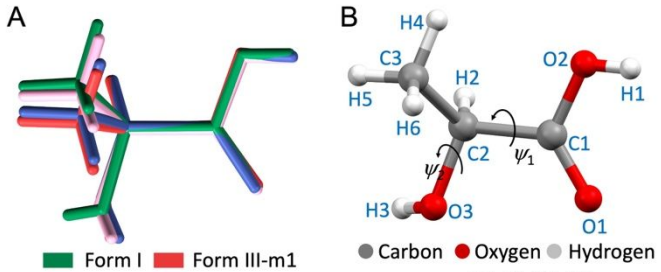

C

(°)	Form I	Form II	Form III-m1	Form III-m2	*SsC*	*AsC*
ψ_1	7.6	-21.2	-23.1	-5.3	-3.0	-18.2
ψ_2	-142.0	53.9	69.3	58.5	0.3	-172.8

Fig. 3 (A) Best fits of four symmetry-independent molecules in Forms **I** (green), **II** (blue), and **III** (pink and red) of LLA. (B,C) Conformational parameters of LLA in three crystal structures and five low energy conformers predicted by quantum chemical calculations. For acronyms of conformations (*SsC, AsC*) see ref.26.

The correspondence of the assembly of molecules in solution and in the crystalline state is important in the clarification of crystal growth mechanisms.[31,32,33] This prompted us to compare the hydrogen bond structure in the newly found LLA polymorphs and the LLA aggregates observed spectroscopically and predicted by quantum chemical computation.[7,8,9,10] $R_2^2(8)$ carboxylic acid dimers are abundant in aqueous solution as evidenced by a combination of computations and vibrational spectra.[7] The self-assembly and solute-solvent hydrogen bonding interactions of LLA in $CDCl_3$, H_2O, and CH_3OH solution were further characterized using experimental FTIR and vibrational circular dichroism (VCD), along with density functional theory calculations.[8] The $R_2^2(8)$ carboxylic-carboxylic dimers are the dominate binary species in solution.

Larger LLA aggregates were considered in cold argon matrices to obviate interactions with solvent molecules.[9] VCD spectra once again identified the $R_2^2(8)$ carboxylic-carboxylic dimers as the main species at 16-24 K, and these dimers are the starting points of most of the higher order (trimers and tetramers) aggregates of LLA and LLA-solvent complexes in DFT calculations (Figure 4D,E).[8,9] However, this most common motif for carboxylic acids was not expressed by any of the three LLA polymorphs (Figure 4A,B,C).

The most recent study of dimerization of LLA in the gas phase, by FTIR spectroscopy,[10] produced no spectra that could reasonably be assigned to any $R_2^2(8)$ carboxylic-carboxylic dimer. While the vapor pressure of a saturated solution of LLA was in principle high enough to produce detectable aggregates, the anticipated concentration was based on a computed equilibrium constant (LLA + LLA ⇌ LLA_2), which may be imperfect according to the authors. Nevertheless, their failure to observe the common dimer[10] is not inconsistent with our failure to see it in crystals.

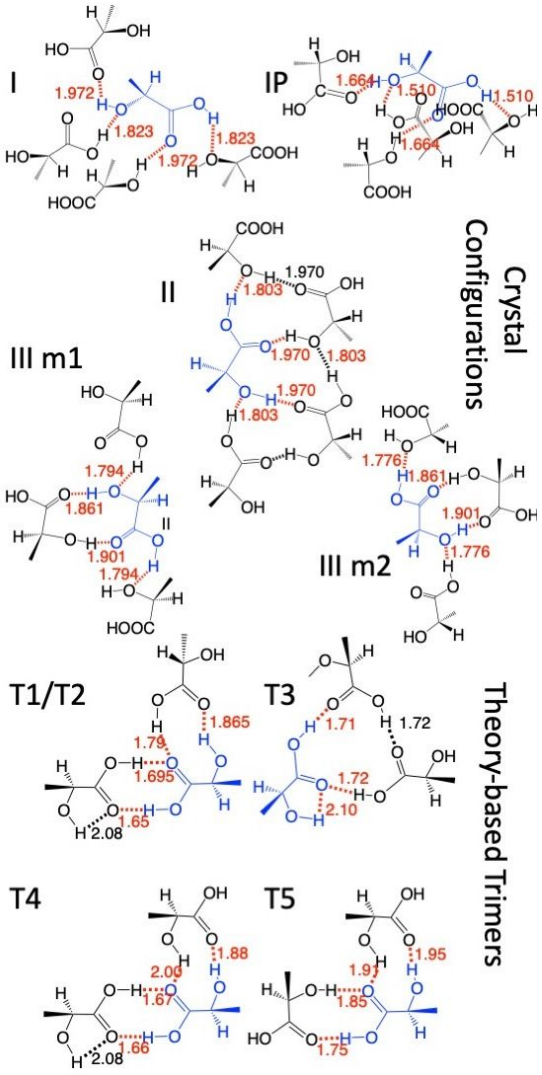

Fig. 4 Summary of hydrogen bonding requirements of single LLA molecules (identified as blue) in trimers and tetramers. H-bonds that satisfy the blue molecule are shown as broken red lines. H-bonds within or between constituent molecules to which the blue molecules are joined are indicated as broken black lines. Top half: Crystal configurations. Experimental structures (**I**, **II**, and **III**) and predicted high pressure phase (**1P**). The independent molecules in **III** are depicted as **III m1** and **III m2**. Crystal aggregates. Bottom half: Theory-based trimers. Most relevant theory-informed trimers matched to vibrational spectra. See e.g. ref (9). T1/T2 represents both trimers T1 and T2 which have different conformations, but the same H-bond configuration. T3 is the only trimer computed without an $R_2^2(8)$ graph set, rather $R_3^3(12)$ albeit no such structures were observed in crystals. T4 and T5 feature $R_2^2(10)$. Other aggregate structures can be found in ref. 9. Only, the H-bonding of blue molecules are complete in these sketches.

Curiously, none of the three ambient structures (**I**-**III**) that we have now are consistent with the aforementioned structures determined by vibrational spectroscopy or quantum chemical computation,[7,8,9,10] suggesting that additional minima for aggregates may be identified in solution or the gas phase, and the other modalities may be found in the solid state. LLA, therefore, underscores how difficult it may be to reason from solution structures to those found in the crystals.[31,32,33] Notwithstanding the strong correspondence between solution and crystal for some carboxylic acid dimers, such as tetrolic acid, it is just as likely, if not more so, that no correspondence is observed, as is the case for racemic mandelic acid**Error! Bookmark not defined.** or tolfenamic acid, for example.[34]

The divergence of supramolecular structures in isotropic media and solid-state structures of LLA indicate that a new starting point, such as the $R_2^2(10)$ dimer structure from Form **III**, or the $R_3^3(11)$ trimer from Form **II**, should be considered for the construction and evaluation of larger LLA aggregates in theoretical calculations.

Notes and references

1 P. Levi, *The Periodic Table*. Schocken Books Inc, New York, 1984.
2 S. Sun, H. Li, J. Chen, Q. Qian, *Physiology*, **2017**, *32*, 453-463.
3 S. Hui, J. M. Ghergurovich, R. J. Morscher., C. Jang, X. Teng, W. Lu, L. A. Esparza, T. Reya, L. Zhan, J. Y. Guo, E. White, *Nature* **2017**, *551*, 115-118.
4 G. A. Brooks, *J. Physiol*. **2001**, *536*, 1.
5 S. M. Ameen, G. Caruso, *Lactic acid in the food industry*. Springer International Publishing AG, Cham, Switzerland, 2017.
6 R. E. Drumright, P.R. Gruber, D.E. Henton, *Adv. Mater.* **2000**, *12*, 1841-1846.
7 Z. Fekete, T. Körtvélyesi, J. Andor, and I. Pálinkó, *J. Mol. Struct.: THEOCHEM* **2003**, *666*, 159-162.
8 M. Losada, H. Tran, Y. Xu, *J. Chem. Phys.* **2008**, *128*, 014508.
9 A. S. Perera, J. Cheramy, M. R. Poopari, Y. Xu, *Phys. Chem. Chem. Phys.* **2018**, *21*, 3574-3584.
10 B. N. Frandsen, A. M. Deal, J. R. Lane, V. Vaida, *J. Phys. Chem. A*, **2021**, *125*, 218–229.
11 H. Benninga, *A history of lactic acid making: a chapter in the history of biotechnology.* Kluwer Academic Publishers, Dordrecht, 1990.
12 H. Borsook, H. M. Huffman, Y. P. Liu, *J. Biol. Chem.* **1933**, *102*, 449-460.
13 D.M.A. Camelot, E.W. Bontenbal, U.S. Patent 7,687,092 (March 30, **2010**).
14 L.A. Tung, C.J. King, *Ind. Eng. Chem. Res.* **1994**, *33*, 3224-3229.
15 B. van Eijck, *J. Mol. Spectrosc.* **1983**, *101*, 133-138.
16 A. Schouten, J.A. Kanters, J. Van Krieken, *J. Mol. Struct.* **1994**, *323*, 165-168.
17 F. Colmenero, *Mater. Adv.*, **2020**, *1*, 1399-1426.
18 S. Chen, I. A. Guzei, L. Yu, *J. Am. Chem. Soc.* **2005**, *127*, 9881-9885.
19 Q. Zhu, A. G. Shtukenberg, D. J. Carter, T. Q. Yu, J. Yang, M. Chen, P. Raiteri, A. R. Oganov, B., Pokroy, I. Polishchuk, P. J. Bygrave, *J. Am. Chem. Soc.* **2016**, *138*, 4881-4889.
20 Y. Su, J. Xu, Q. Shi, L. Yu, T. Cai, *Chem. Commun.* **2018**, *54*, 358-361.
21 J. Yang, B. Erriah, C. T. Hu, E. Reiter, X. Zhu, V. López-Mejías, I. P. Carmona-Sepúlveda, M. D. Ward, B. Kahr, *Proc. Natl. Acad. Sci. U. S. A.,* **2020**, *117*, 26633-26638.
22 K. Zhang, N. Fellah, A. G. Shtukenberg, X. Fu, C. Hu M. D. Ward, *CrystEngComm*. **2020**, *22*, 2705-2708.
23 X. Ou, X. Li, H. Rong, L. Yu, M. Lu, *Chem. Commun.* **2020**, *56*, 9950-9953.
24 X. Li, X. Ou, B. Wang, H. Rong, B. Wang, C. Chang, B. Shi, L. Yu, M. Lu, *Commun. Chem.* **2020**, *3*, 1-8.
25 M. Pecul, A. Rizzo, J. Leszczynski, *J. Phys. Chem. A* **2002**, *106*, 11 008-11016.
26 A. Borba, A. Gómez-Zavaglia, L. Iapinski, R. Fausto, *Phys. Chem. Chem. Phys.* **2004**, *6*, 2101-2108.
27 A. Smaga, J. Sadlej, *J. Phys. Chem. A*, **2010**, *114*, 4427-4436.
28 M. C. Etter, J. C. MacDonald, J. Bernstein, *Acta Cryst. B* **1990**, *46*, 256-262.
29 J. Bernstein, R. E. Davis, L. Shimoni, N. L. Chang, *Angew. Chem. Int.* **1995**, *34*, 1555-1573.
30 E. C. Escudero-Adán, J. Benet-Buchholz, P. Ballester, *Acta. Crystallogr. Sect. B* **2014**, *70*, 660-668.
31 J. Huang, T. C. Stringfellow, L. Yu, *J. Am. Chem. Soc.* **2008**, *130*, 13973-13980.
32 R. J. Davey, S. L. Schroeder, J. H. ter Horst, *Angew. Chem. Int. Ed.* **2013**, *52*, 2166-2179.
33 W. Du, A. J. Cruz-Cabeza, S. Woutersen, R. J. Davey, Q. Yin, *Chem. Sci.* **2015**, *6*, 3515-3524.
34 W. Du et al. *Chem. Sci.* **2015**, *6*, 3515-3524.